

(α, d) reaction on ^{12}C and ^{13}C and weak coupling configurations

M. Yasue,* J. J. Hamill,[†] H. C. Bhang,[‡] M. A. Rumore, and R. J. Peterson

Nuclear Physics Laboratory, University of Colorado, Boulder, Colorado 80309

(Received 13 March 1984)

Cross sections for the (α, d) reaction on ^{12}C and ^{13}C were measured at $E_\alpha = 34.9$ MeV in the range of excitation energies up to 11 MeV in ^{14}N and up to 13 MeV in ^{15}N . The angular distributions were compared to calculations with the zero-range distorted-wave Born approximation with the assumption of a deuteron-cluster transfer. On the basis of the assumption that the transferred two nucleons are weakly coupled to the target nuclei, correspondences between the transferred angular momenta and the strengths for the two-nucleon pairs were found for the residual nuclei ^{14}N and ^{15}N . Effects of the $0d_{3/2}$ shell and a necessity for the tensor force are discussed in terms of the two-nucleon configurations $d_{3/2}p_{1/2}$ and $(d_{5/2})^2$, respectively.

I. INTRODUCTION

The ^{15}N nucleus has been studied theoretically and experimentally by many authors. These works are compiled in Ref. 1. In a simple shell model description for the ^{15}N nucleus, the low-lying negative parity states correspond to a single hole in the $0p_{1/2}$ or $0p_{3/2}$ shell and the low-lying positive parity states correspond to a single particle in the $1s_{1/2}$ or $0d_{5/2}$ shell coupled to two holes in the $0p$ shell. Recently, Kretschmer *et al.*² performed the $^{14}\text{N}(d, p)^{15}\text{N}$ reaction and compared their results with various shell model calculations. Their findings are the following: (1) The states of ^{15}N below 8 MeV in excitation energy have simple configurations, rather close to the simple $j-j$ coupling model. (2) Above the excitation energy of 8 MeV, a $0d_{3/2}$ transfer contributes to the reaction and the spectroscopic strengths deviate considerably from the description of the simple $j-j$ coupling model. (3) The best overall agreement seems to be with the weak coupling approach of Lie, Engeland, and Dahll.³

Above 8 MeV in excitation energy, beside the contribution of the $0d_{3/2}$ shell, the effect of the configuration of $(1s0d)^2(0p)^{-3}$ will appear as predicted by the weak coupling shell model.³ Examples of such a configuration are the 13.00 MeV, $\frac{11}{2}^-$ and 11.94 MeV, $\frac{9}{2}^-$ states in ^{15}N . Their predictions³ for these states are the following:

(1) The $\frac{11}{2}^-$ state is the stretched state with a configuration

$$[(0d_{5/2})^2_{5+}(0p_{1/2})^{-3}_{1/2-}]_{11/2-}.$$

(2) There should be two $\frac{9}{2}^-$ states with configurations

$$[(0d_{5/2})^2_{5+; T=0}(0p_{1/2})^{-3}_{1/2-}]_{9/2-}$$

and

$$[(0d_{5/2})^2_{4+; T=1}(0p_{1/2})^{-3}_{1/2-}]_{9/2-}.$$

The strengths of these two configurations are nearly equally distributed between the two lowest $\frac{9}{2}^-$ states.

These $\frac{11}{2}^-$ and $\frac{9}{2}^-$ states have relatively pure configurations. Therefore they would provide a good chance for investigation of the validity of the weak coupling shell

model to the highly-excited states in ^{15}N . The 13.00 MeV $\frac{11}{2}^-$ state and the 11.94 MeV $\frac{9}{2}^-$ state have been previously observed by the $^{13}\text{C}(\alpha, d)^{15}\text{N}$ reaction⁴ at $E_\alpha = 40.1$ MeV and by the $^{13}\text{C}(^6\text{Li}, \alpha)^{15}\text{N}$ reaction⁵ at $E_{^6\text{Li}} = 32.0$ MeV. These reactions require $\Delta T = 0$ transfer, so that only the

$$[(0d_{5/2})^2_{5+}(0p_{1/2})^{-3}_{1/2-}]_{9/2-}$$

configurations of the $\frac{9}{2}^-$ states are to be observed in these reactions. As the target nucleus ^{13}C has a relatively pure $(0p_{1/2})^{-3}_{1/2-}$ configuration,⁶ it is expected in the model³ that the (α, d) and ($^6\text{Li}, \alpha$) reactions on ^{13}C will excite each of the $\frac{9}{2}^-$ states with an enhancement factor half of that for the $\frac{11}{2}^-$ state. Contrary to the above estimation, Harwood and Kemper⁵ observed in the $^{13}\text{C}(^6\text{Li}, \alpha)^{15}\text{N}$ reaction that the enhancement factor for the 11.94 MeV $\frac{9}{2}^-$ state is twice as large as that for the $\frac{11}{2}^-$ state. On the other hand, the $^{13}\text{C}(\alpha, d)^{15}\text{N}$ reaction reported by Lu *et al.*⁴ seems to have transfer strengths for the $\frac{9}{2}^-$ and $\frac{11}{2}^-$ states as predicted by the above estimation, although they did not compare the experimental angular distributions for the $\frac{9}{2}^-$ and $\frac{11}{2}^-$ states with DWBA calculations. Thus, these experimental data show a discrepancy of a factor of 4 for the ratio of the enhancement factors for the $\frac{9}{2}^-$ and $\frac{11}{2}^-$ states which are considered to have relatively simple configurations in the weak coupling shell model. Besides, contrary to the prediction, another $\frac{9}{2}^-$ state was not found experimentally. Recently, these highly excited states in ^{15}N have also been studied via three nucleon transfer reactions such as (α, p) and ($^7\text{Li}, \alpha$) reactions.⁷⁻⁹ A candidate for the other $\frac{9}{2}^-$ state was proposed by Hamill *et al.*⁷ via the $^{12}\text{C}(\alpha, p)^{15}\text{N}$ reaction to be the 12.56 MeV state. However, the state has not yet been investigated via a two-nucleon transfer reaction, which is considered to be suited to see a two-particle state in comparison to the three nucleon transfer reaction. Another important prediction by the weak coupling model³ is a distribution of the strength of the $0d_{3/2}$ single particle above $E_x = 8$ MeV in ^{15}N . Hitherto only slight fragments

of the strength have been observed below $E_x = 9$ MeV by Kretschmer *et al.*² via the $^{14}\text{N}(d, p)^{15}\text{N}$ reaction, but the main component is not found experimentally. In order to understand the nature of ^{15}N in these excitation energies, further experimental studies are needed.

On the other hand, more detailed studies¹⁰⁻¹³ on two-nucleon transfer reactions such as (α, d) , $(^3\text{He}, p)$, and $(^6\text{Li}, \alpha)$ have been carried out on the target nucleus ^{12}C . Fairly good correspondences^{10,11} between the experimental data and the weak coupling shell model calculation¹⁴ for ^{14}N are found up to 10 MeV in the excitation energy of ^{14}N . It is expected that the comparison of the experimental strengths for the two-nucleon transfer reaction on ^{12}C and ^{13}C would provide a clue as to the structure of these states in ^{15}N . Hitherto detailed comparison of the reaction on these two targets has scarcely been reported. In this paper, by applying an assumption of the weak coupling of two transferred nucleons with target nuclei to the study of the $^{12}\text{C}(\alpha, d)^{14}\text{N}$ and $^{13}\text{C}(\alpha, d)^{15}\text{N}$ reactions, configurations of the states in ^{15}N are discussed in compar-

ison with those in ^{14}N , with an emphasis on high spin states favored by the reaction kinematics.

II. EXPERIMENTAL PROCEDURE AND RESULTS

The experiment was performed with the 34.9-MeV α beam from the University of Colorado AVF cyclotron. A natural carbon foil of 0.08 ± 0.01 mg/cm² in thickness and a 98% enriched ^{13}C foil of 0.29 ± 0.03 mg/cm² in thickness were used for the targets. The target thickness was calibrated by an ^{241}Am alpha thickness gauge. Reaction products were detected by a counter telescope (ΔE , 50 μm ; E , 5 mm) which was cooled to -29°C by an alcohol cooling system. Particles were identified by using an on-line computer. Typical deuteron spectra at $\theta_{\text{lab}} = 10^\circ$ are shown in Fig. 1, where the measured energy resolutions are 50 and 60 keV FWHM for the $^{12}\text{C}(\alpha, d)^{14}\text{N}$ and $^{13}\text{C}(\alpha, d)^{15}\text{N}$ reactions, respectively. To resolve the adjacent doublet at $E_x = 5.27$ and 5.30 MeV in ^{15}N , yields for the $^{13}\text{C}(\alpha, d)^{15}\text{N}$ reaction were also mea-

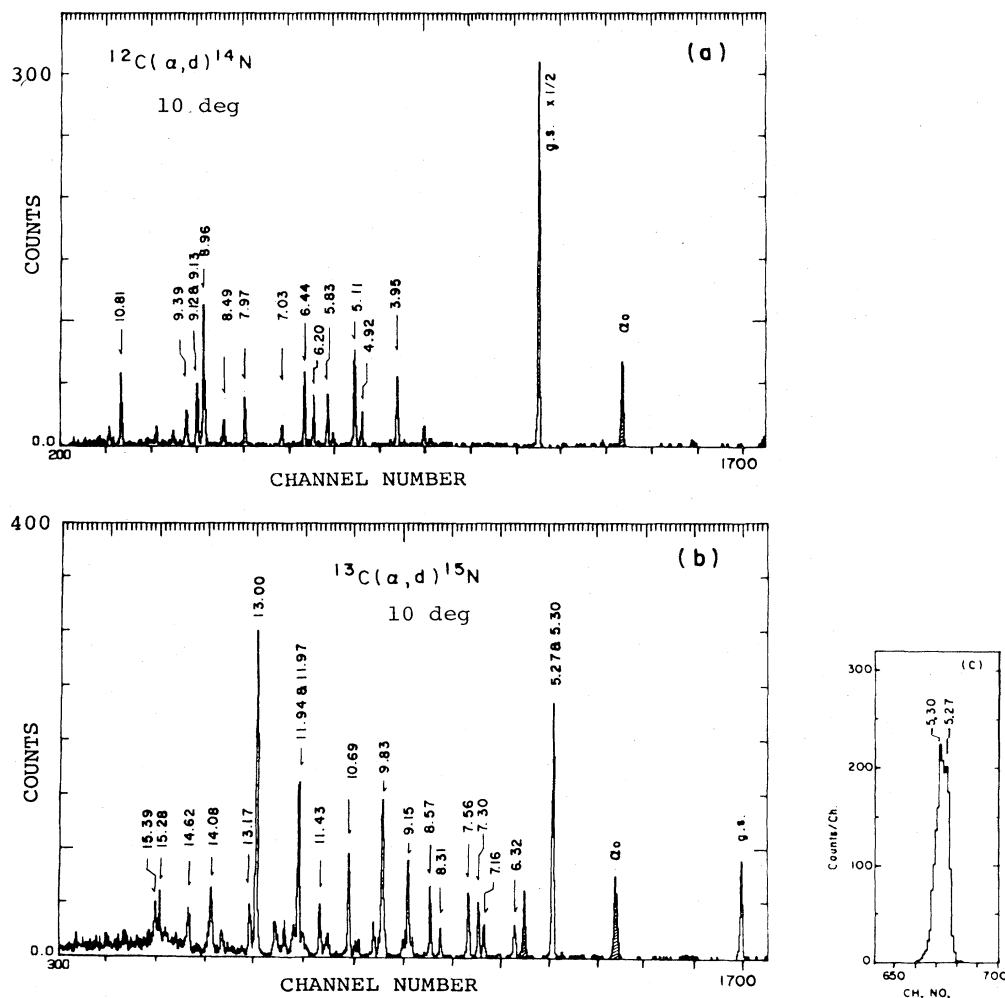


FIG. 1. Typical energy spectra for (a) $^{12}\text{C}(\alpha, d)^{14}\text{N}$ and (b) $^{13}\text{C}(\alpha, d)^{15}\text{N}$ reactions at $E_\alpha = 34.9$ MeV, $\theta_{\text{lab}} = 10^\circ$. (c) A portion of the 5.27 and 5.30 MeV doublet in the spectrum for the $^{13}\text{C}(\alpha, d)^{15}\text{N}$ reaction, which was measured with a spectrometer. Peaks with a suffix α_0 are due to the elastic scattering of alpha particles. A hatched peak near $E_\alpha = 6.32$ MeV in (b) is due to the reaction $^{12}\text{C}(\alpha, d)^{14}\text{N}(\text{g.s.})$.

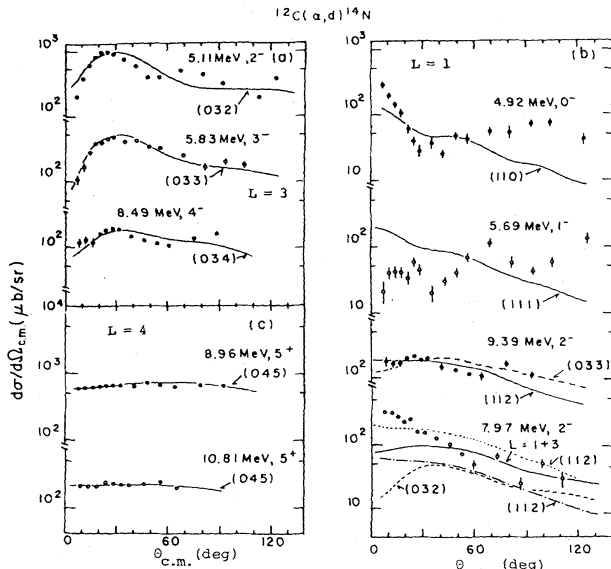


FIG. 2. Closed and open circles are angular distributions for the $^{12}\text{C}(\alpha,d)^{14}\text{N}$ reaction at $E_\alpha=34.9$ MeV. Curves are results of zero-range DWBA calculations with NLJ values as shown in the figure. Figures are sorted to groups (a), (b), and (c) according to the leading contribution in the transferred angular momenta $L=3, 1,$ and $4,$ respectively.

sured with a spectrometer system.¹⁵ A spectrum for the doublet is shown in Fig. 1(c), where the energy resolution is 35 keV FWHM. The doublet was analyzed by using the peak-fitting program SPECTR.¹⁶ A peak at $E_x=15.28$ MeV in ^{15}N was previously assigned to a contaminant due to the 8.96 MeV state in ^{14}N .⁴ However, the contribution of the contaminant is estimated to be at most 25% of the total yield for the peak by comparing the spectra for ^{14}N and ^{15}N . Some of the obtained angular distributions are shown in Figs. 2–4. Errors in absolute cross sections are estimated to be less than 15%. The relative strength for transitions on the two targets is known to an accuracy of $\pm 5\%$. The whole of the result is represented in Ref. 17.

III. ANALYSES

In the (α,d) reaction, the deuteron-cluster transfer model for the transition leading to states with simple two-nucleon configurations is reported by de Meijer *et al.*¹⁸ to be in good agreement with the results calculated by using microscopic two nucleon form factors. The usefulness of the cluster model in the (α,d) reaction has been demonstrated by several authors^{18,19} for the transition to the states with simple configurations in sd -shell nuclei.

Our present concern is to compare the distributions of the transferred angular momenta and the cross-section strengths for the $^{13}\text{C}(\alpha,d)^{15}\text{N}$ reaction with those for the $^{12}\text{C}(\alpha,d)^{14}\text{N}$ reaction by assuming simple transferred two-nucleon configurations such as $(p)^2$, $(sd)^2$, and $(p)(sd)$. In the present work, calculations are carried out by using the program DWUCK 4 (Ref. 20) in the framework of the zero-range DWBA on an assumption of

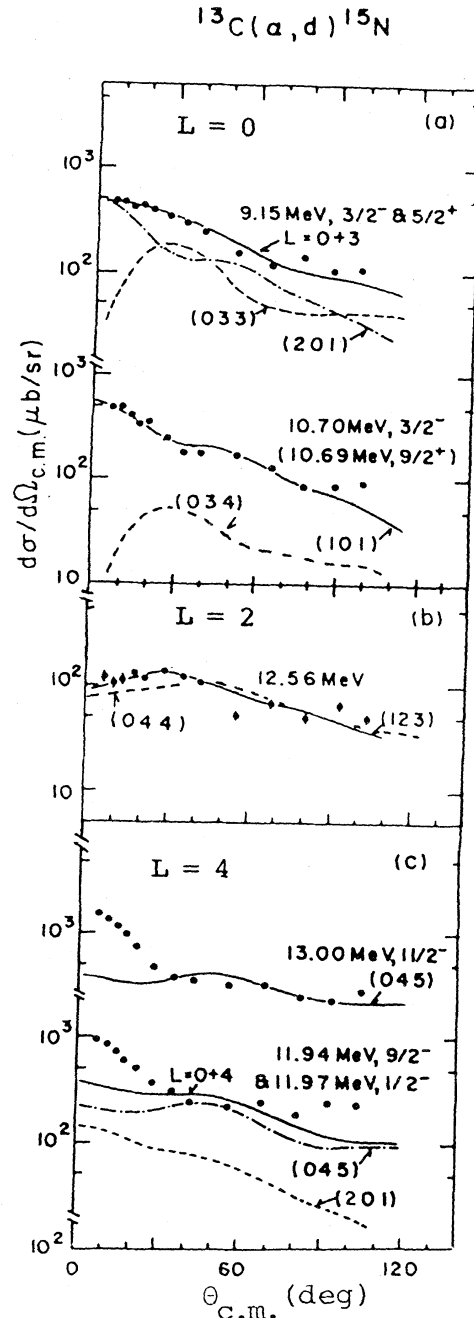


FIG. 3. Angular distributions for the $^{13}\text{C}(\alpha,d)^{15}\text{N}$ reaction at $E_\alpha=34.9$ MeV. See also the caption to Fig. 2.

deuteron cluster transfer.

For harmonic-oscillator radial wave functions, the relation between the quantum numbers for the relative (ν,λ) and c.m. motion (N,L) of the cluster and those for the individual nucleons (n_i,l_i) is given by

$$2(\nu+N)+\lambda+L=2(n_1+n_2)+l_1+l_2. \quad (1)$$

It is commonly assumed that Eq. (1) is also valid for Woods-Saxon wave functions. Assuming that the two nucleons are in a $0s$ state in the deuteron cluster, Eq. (1) can be approximated to

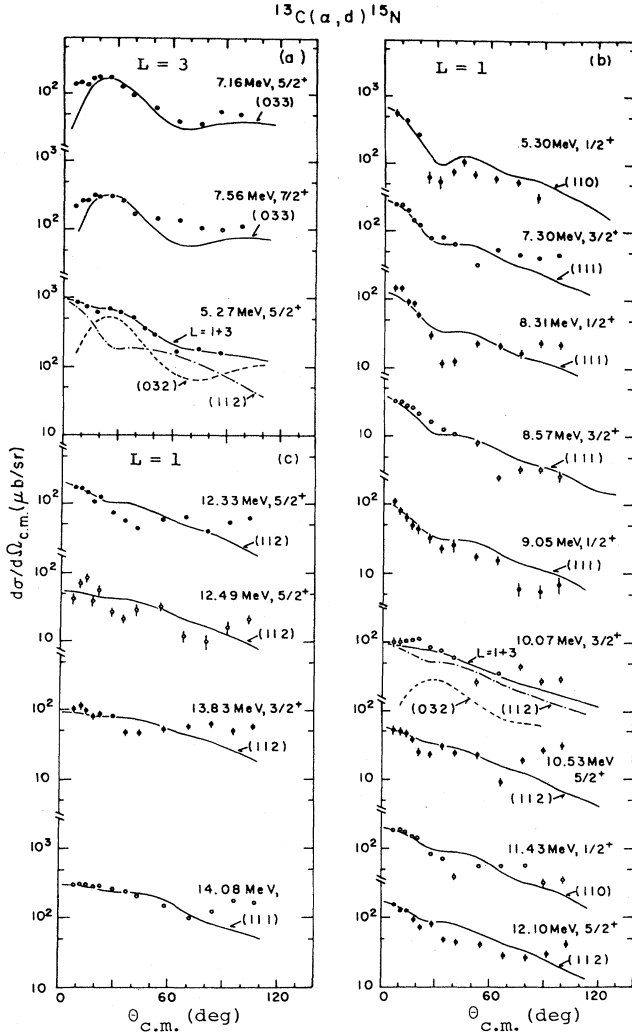


FIG. 4. Angular distributions for the $^{13}\text{C}(\alpha, d)^{15}\text{N}$ reaction at $E_\alpha = 34.9$ MeV. See also the caption to Fig. 2.

$$2N + L = 2(n_1 + n_2) + l_1 + l_2. \quad (2)$$

The number of radial nodes, N (excluding those at $r=0$ and $r=\infty$), and the orbital angular momentum, L , of the transferred cluster have a relation with the values $(2n_i + l_i)$ of each transferred nucleon. Thus, the form factor of the cluster is insensitive to the detailed full angular momentum properties of the wave functions of the transferred nucleons, such as $0d_{5/2}$, $0d_{3/2}$, or $1s_{1/2}$. We label these together as (sd) .

Optical model potential parameters for the initial and the final channels are cited from Refs. 21 and 22. These parameters satisfy the well-matching condition²³ between the channels, and are listed in Table I. The parameters for alpha particles in Table I were found⁷ to fit the data well for the elastic scattering of alpha particles from ^{12}C and ^{13}C at $E_\alpha = 35$ MeV.

As discussed in other works,^{18,24} the calculated cross section for the (α, d) reaction is expressed by the formula

$$\sigma_{\text{cal}} = N \frac{3}{2} \frac{2J_F + 1}{2J_I + 1} \frac{\sigma_{\text{DWUCK}}}{2J + 1}, \quad (3)$$

TABLE I. Parameters of optical model potential and bound states used in the program DWUCK 4 (Ref. 20) for the (α, d) reaction on ^{12}C and ^{13}C at $E_\alpha = 34.9$ MeV. Parameters refer to the Woods-Saxon shape and its derivatives.

	α^a	d^b	Bound d
V_R (MeV)	-217	-82.5	c
r_R (fm)	1.3	1.2	1.2
a_R (fm)	0.58	0.75	0.75
W_V (MeV)	-28		
$4W_D$ (MeV)		31.2	
r_W (fm)	1.5	1.32	
a_W (fm)	0.32	0.84	
$2V_{1s}$ (MeV)		-11.26	
r_{1s} (fm)		0.92	
a_{1s} (fm)		1.0	
r_c (fm)	1.25	1.25	1.25

^aReference 21.

^bReference 22.

^cAdjusted to give the deuteron binding energy. For unbound states, form factors loosely bound by 0.1 MeV were used.

where the notations are the same as in Refs. 18, 20, and 24. N is a normalization factor, whose value is set to 20 in the present calculation according to the results in other work.^{18,24} The ratio of experimental cross sections to calculated ones,

$$R = \left[\frac{d\sigma}{d\Omega} \right]_{\text{exp}} / \left[\frac{d\sigma}{d\Omega} \right]_{\text{cal}}, \quad (4)$$

reflects the nature of the transferred two-nucleon configuration and the nature of the target nuclei. Calculated angular distributions are shown in Figs. 2–4 with NLJ values as assumed for the transitions. If two values of the angular momenta contribute to an (α, d) transition, the angular distribution for the transition is fitted by the two sets of calculated curves with the allowed L values. The calculated curves are normalized to the data at forward angles. The obtained normalizations, the so-called enhancement factors R in Eq. (4), are listed in Tables II and III.

IV. DISCUSSION

Details of the obtained results will be given elsewhere.¹⁷ In the subsequent subsections, characteristic states observed in the present (α, d) reaction on ^{12}C and ^{13}C are discussed.

A. Two-nucleon configurations of $(p)(sd)$ in ^{14}N and ^{15}N

In ^{14}N , eight $T=0$ states with negative parity are known below $E_x = 11$ MeV.¹ Cross sections for all of them have been obtained in the present $^{12}\text{C}(\alpha, d)^{14}\text{N}$ reaction, except for the 9.13 MeV 2^- state, which is not separated from the adjacent 9.12 MeV 3^+ state. Figure 2(a) shows the cross sections for the $L=3$ transitions leading to the 2^- , 5.11 MeV, the 3^- , 5.83 MeV, and the 4^- , 8.49 MeV states in ^{14}N . The latter two transitions are of pure $L=3$ transfer, and their main configurations are

TABLE II. States of ^{14}N and ^{15}N observed in the (α, d) reaction at $E_\alpha = 34.5$ MeV, primarily of $(p)(sd)$ structure. The integrated cross section for the 9.13 MeV state is estimated from the total yields for the 2^- , 9.13 MeV and the 3^+ , 9.12 MeV states by referring to the strengths of the angular momentum transfer $L = 1$ and 2. Those for the 9.15 MeV $\frac{5}{2}^+$ and $\frac{3}{2}^-$ states are also estimated by referring to the $L = 3$ and 0 strengths in the angular distributions for these states. The J^π value marked with an asterisk is proposed in the present work. For cases of the transfer values NLJ , separate enhancement factors are listed for both terms. Integrated cross sections are over the angles $\theta_{c.m.} = 7^\circ - 100^\circ$ and those with suffix a are over the angles $\theta_{c.m.} = 7^\circ - 90^\circ$.

Main two-nucleon configuration	Nucleus	E_x (MeV)	J^π	σ_{int} (mb)	Transferred NLJ	$R = \frac{\sigma_{\text{exp}}}{\sigma_{\text{cal}}}$
$p_{1/2}s_{1/2}$	^{14}N	4.92	0^-	0.53	110	0.26
	^{15}N	5.30	$\frac{1}{2}^+$	0.53	110	0.53
$p_{1/2}d_{5/2}$	^{14}N	5.11	2^-	4.56	032	1.2
	^{15}N	5.27	$\frac{5}{2}^+$	2.04	032 + 112	0.46, 0.27
$p_{1/2}s_{1/2}$	^{14}N	5.69	1^-	0.62	111	0.20
	^{15}N	7.30	$\frac{3}{2}^+$	0.42	111	0.17
	^{15}N	8.31	$\frac{1}{2}^+$	0.15	111	0.20
$p_{1/2}(sd)$	^{15}N	8.57	$\frac{3}{2}^+$	0.56	111	0.33
$p_{1/2}s_{1/2}$	^{15}N	9.05	$\frac{1}{2}^+$	0.13	111	0.21
$p_{1/2}d_{5/2}$	^{14}N	5.83	3^-	2.6	033	0.59
	^{15}N	7.16	$\frac{5}{2}^+$	0.49	033	0.22
	^{15}N	7.56	$\frac{7}{2}^+$	1.06	033	0.36
	^{15}N	9.15	$\frac{5}{2}^+$	0.57	033	0.33
$p_{3/2}s_{1/2}$	^{14}N	7.97	2^-	0.60	112 + 032	0.14, 0.14
	^{15}N	10.07	$\frac{3}{2}^+$	0.37	112 + 032	0.17, 0.10
	^{15}N	10.53	$\frac{5}{2}^+$	0.19	112	0.12
$p_{3/2}d_{5/2}$	^{14}N	8.49	4^-	1.09	034	0.50
	^{15}N	10.69	$\frac{9}{2}^+$			
$p_{3/2}d_{5/2}$	^{14}N	9.13	2^-	0.32 ^a	112	0.33
	^{15}N	12.10	$\frac{5}{2}^+$	0.37	112	0.19
$p_{1/2}d_{3/2}$	^{14}N	9.39	$(2^-)^*$	0.92 ^a	112	0.21
	^{15}N	12.33	$\frac{5}{2}^+$	0.44	112	0.19
	^{15}N	13.83	$\frac{3}{2}^+$	0.45	112	0.28

$(p_{1/2}d_{5/2})_{3^-}$ and $(p_{3/2}d_{5/2})_{4^-}$.¹⁴ On the other hand, the transferred angular momentum $L = 1$ is also allowed for the transition to the 5.11 MeV state. The angular distribution for the 2^- , 5.11 MeV state shows a more diffractive pattern than calculated with $L = 3$ transfer, indicating interference between $L = 1$ and 3 transfers. In the $^{12}\text{C}(^3\text{He}, p)^{14}\text{N}$ reaction¹¹ at the lower incident energy of $E = 20$ MeV, where lower transferred angular momenta are preferred, the cross section for the 5.11 MeV state represents an $L = 1$ type of shape. Although the 5.11 MeV state is simply of a $(p_{1/2}d_{5/2})_{2^-}$ configuration in the shell model calculation,¹⁴ it is to be noticed that the dominant pattern in the angular distribution is different for

the (α, d) and $(^3\text{He}, p)$ reactions.

The (α, d) transition to the 0^- , 4.92 MeV and the 1^- , 5.69 MeV states go by $L = 1$ transfer. In the $^{12}\text{C}(^3\text{He}, p)^{14}\text{N}$ reaction,¹¹ the shapes of the angular distributions for the 0^- and 1^- states are well reproduced by the DWBA calculations with $L = 1$ transfer. In the present (α, d) reaction, where angular momentum transfer $L = 3$ is preferred, the shapes show large deviations from the calculated curves with $L = 1$ transfer, as seen in Fig. 2(b). Further discussion on the transition to the 1^- state will be given in Sec. IV C. The 2^- , 7.97 MeV state also shows considerable deviation from the calculated curves, as seen in Fig. 2. The weak coupling shell model calcula-

TABLE III. High-spin states of ^{14}N and ^{15}N observed in the (α, d) reaction at $E_\alpha = 34.5$ MeV.

Main two-nucleon configurations	Nucleus	E_x (MeV)	J^π	σ_{int} (mb)	Transferred	
					NLJ	$R = \frac{\sigma_{\text{exp}}}{\sigma_{\text{cal}}}$
$(d_{5/2})^2$	^{14}N	8.96	5^+	5.12	045	1.7
	^{15}N	11.94	$\frac{9}{2}^-$	2.03	045	0.50
	^{15}N	13.00	$\frac{11}{2}^-$	2.66	045	0.80
$(d_{5/2})^2$	^{14}N	10.81	5^+	0.97 ^a	045	1.4 ^b
$(sd)^2$	^{15}N	12.56	c	0.64	123	0.18

^aIntegrated cross sections are over the angles $\theta_{\text{c.m.}} = 7^\circ - 90^\circ$.

^bThe factor is obtained with a form factor loosely bound by 0.1 MeV.

^cThe spin parity for the 12.56 MeV state is proposed as $J^\pi = \frac{9}{2}^-$ in Ref. 7. See also the caption to Table II.

tion of Lie¹⁴ describes the 7.97 MeV state as having a configuration of $p_{3/2}d_{5/2}$. If so, a two-step process via the 2^+ state in ^{12}C , which has a large component for a $p_{1/2}p_{3/2}$ configuration, will be allowed in the (α, d) transition to the 7.97 MeV state. Thus, the observed deviation in the angular distribution for the 7.97 MeV state may come from the interference in the reaction processes.

Lie also predicted the existence of another 2^- state with a configuration of $p_{1/2}d_{3/2}$. For a state with such a configuration, the two-nucleon transfer reaction as well as the one-nucleon transfer reaction will show a simple angular distribution as predicted by the DWBA calculations. The recent compilation lists the spin-parity for the 9.39 MeV state as $J^\pi = 2^-$ or 3^- ,¹ so this state is a candidate for the 2^- state with the $p_{1/2}d_{3/2}$ configuration. The angular distribution for this state is reproduced well by the $(NLJ) = (112)$ curve, not by the $(NLJ) = (033)$ as seen in Fig. 2(b). Previously, the 9.39 MeV state was proposed to be of the form $(p_{3/2}d_{5/2})_{3^-}$ by Lie.¹⁴ In the (α, d) reaction, the transition to a 3^- state with such a configuration is hindered by a factor of about 20 due to the Clebsch-Gordan coefficient for the spin summation compared to

that to the 3^- , 5.83 MeV state of the $(p_{1/2}d_{5/2})$ configuration. The experimental ratio of the strength for the 9.39 MeV state to that for the 5.83 MeV state is as much as $\frac{1}{3}$. Thus, assignment of the $(p_{3/2}d_{5/2})_{3^-}$ configuration to the 9.39 MeV state is ruled out. Table IV is a comparison of spectroscopic strengths for the (α, d) transition to the 2^- states in ^{14}N with those for the $^{13}\text{C}(^3\text{He}, d)^{14}\text{N}$ reaction, which was carried out by Peterson and Hamill.²⁵ The shell model calculation¹⁴ proclaims the existence of four 2^- states, each of which has a configuration as listed in Table IV. Key points to locate the 2^- state with the $p_{1/2}d_{3/2}$ configuration are the following:

(1) The (α, d) transition to such a state has a strength proportional to that in the $(^3\text{He}, d)$ transition, because in the latter transition the strengths for the $p_{3/2}(sd)$ configuration should be much smaller owing to the small component of the $p_{3/2}$ hole configuration in the wave function of ^{13}C .

(2) The 2^- state with the $p_{1/2}d_{3/2}$ configuration should be highest in excitation energy of these 2^- states according to the prediction.¹⁴

From the above two points of view, our proposal is that

TABLE IV. Spectroscopic information on the 2^- states in ^{14}N .

E_x (MeV)	Spectroscopic strength		Lie's prediction ^c	
	$(\alpha, d)^a$	$(^3\text{He}, d)^b$	Main configuration	E_x (MeV)
5.11	1.2	0.36	$p_{1/2}d_{5/2}$	5.12
	(1.0)	(1.0)		
7.97	0.28	0.015	$p_{3/2}s_{1/2}$	8.28
	(0.24)	(0.04)		
9.13	0.33	0.028	$p_{3/2}d_{5/2}$	9.32
	(0.28)	(0.08)		
9.39	0.21	0.12	$p_{1/2}d_{3/2}$	11.1
	(0.18)	(0.33)		

^aEnhancement factor in the present work.

^bSpectroscopic factor in the $^{13}\text{C}(^3\text{He}, d)^{14}\text{N}$ reaction at $E_{\text{lab}} = 43.6$ MeV, cited from the work by Peterson and Hamill (Ref. 25).

^cReference 14. Spectroscopic strengths in parentheses are those normalized to the value for the 5.11 MeV state.

the 9.39 MeV state in ^{14}N has a configuration of $(p_{1/2}d_{3/2})_{2-}$. This is the first finding of a large $d_{3/2}$ component in the highly excited states of ^{14}N . Previously, only small fragments of the $0d_{3/2}$ shell were known below $E_x=9$ MeV by the (d,p) reaction.²

We now compare these structures in ^{14}N to the two-nucleon data for ^{15}N . Previously, Pedersen *et al.*²⁶ studied the states of ^{15}N by use of the reaction $^{13}\text{C}(^3\text{He},p)^{15}\text{N}$ at $E_{\text{lab}}=20$ MeV. In their work, the angular distributions for the 7.16, 7.30, 7.56, 9.05, and 10.07 MeV states with positive parity showed shapes much different from the calculated curves. They proposed two-step processes via inelastic scattering in the initial channel in order to explain the interferencelike structures found in the experimental angular distributions. As referred to in the preceding paragraph and treated in Sec. IV C, the present (α,d) reaction is also apt to reflect such effects on the shapes of the angular distributions. Thus one may also expect some deviations of the calculated curves from the angular distributions for the (α,d) transition to these states. As seen in Fig. 4, however, the calculated curves show reasonable fits to the data. Hence the cause of the deviation observed in the $^{13}\text{C}(^3\text{He},p)^{15}\text{N}$ reaction should be sought elsewhere.

In the weak coupling model of Lie, Engeland, and Dahll,³ it is pointed out that the positive parity states in ^{15}N have some mixtures of configurations of 1p-2h and 3p-4h. In the $^{13}\text{C}(^3\text{He},p)^{15}\text{N}$ reaction at a lower incident energy, a knock-on process may also play an important role for transitions to the states with 3p-4h configurations in ^{15}N . Apart from such ambiguities of the reaction process in the $(^3\text{He},p)$ transfer, the reasonable fits of the calculations to the present data for the (α,d) transition to the positive parity states in ^{15}N indicate the usefulness of the (α,d) transition for deducing spectroscopic information on the 1p-2h character in ^{15}N .

In their calculation,³ four $\frac{1}{2}^+$ states are predicted in ^{15}N below $E_x=10.33$ MeV: The 8.31 and 9.05 MeV $\frac{1}{2}^+$ states have configurations $(s_{1/2})(p_{1/2})_{1+;0}^{-2}$ and $(s_{1/2})(p_{1/2})_{0+;1}^{-2}$, respectively, while the 5.30 and 11.43 MeV $\frac{1}{2}^+$ states have rather complex configurations, a mixture of 1p-2h and 3p-4h structures. The $\frac{1}{2}^+$, 5.30 MeV state is expected to be only weakly excited by a two-nucleon stripping reaction due to its dominant 3p-4h structure.³ The cross section for the two-nucleon transfer to the 5.30 MeV state has been obtained for the first time in the present work. Contrary to the speculation, our new data for the 5.30 MeV state show larger strength than found for the 8.31 and 9.05 MeV states as listed in Table II. The large enhancement factor for the 5.30 MeV state means a stronger mixture of the 1p-2h configuration to their mainly 3p-4h configuration than predicted in the weak coupling model, thus suggesting a weak point of the model in handling the $1s_{1/2}$ nucleon in ^{15}N . The $1s_{1/2}$ single particle wave function is expected to be sensitive to np - mh configurations, because of its radial node near the nuclear surface.

Previously, Harwood and Kemper²⁷ measured the γ -decay strengths of the ^{15}N states via $^{12}\text{C}(^7\text{Li},\alpha\gamma)$, $^{12}\text{C}(^6\text{Li},^3\text{He}\gamma)$, and $^{11}\text{B}(^7\text{Li},t\gamma)$ reactions and compared

the strengths to those predicted by the weak-coupling shell model.³ They also pointed out the insufficiency of the model to describe the electromagnetic properties of the $\frac{1}{2}^+$ states of ^{15}N . Thus, the present results for the $\frac{1}{2}^+$ states as well as the work by Harwood and Kemper indicate a necessity for a more detailed treatment of the $1s_{1/2}$ state in ^{15}N . Actually, Millener and Kurath²⁸ found the need for noncentral components in the particle-hole interactions to describe the $1s_{1/2}$ orbit in p -shell nuclei, and excellently explained the experimental result for the β decay of ^{14}B .

In the weak coupling shell model calculation,³ the $\frac{3}{2}^+$ states at $E_x=7.30$, 8.57, and 10.07 MeV, and the $\frac{5}{2}^+$ states at $E_x=5.27$, 7.16, and 9.15 MeV are of 1p-2h type of configurations such as $s_{1/2}(p_{1/2})^{-2}$ and $d_{5/2}(p_{1/2})^{-2}$. The enhancement factors for the $\frac{3}{2}^+$ states are similar to each other as predicted by the calculation.³ Those for the $\frac{5}{2}^+$ states at $E_x=5.27$, 7.16, and 9.15 MeV are predicted to be in the ratio of about 2:1:1, respectively. The experimental data for the $\frac{5}{2}^+$ states also show such ratios. Thus, the calculation can explain all the strengths for the (α,d) transition to these $\frac{3}{2}^+$ and $\frac{5}{2}^+$ states. Furthermore, the calculation predicts the existence of another pair of $\frac{3}{2}^+$ and $\frac{5}{2}^+$ states with a configuration of $d_{3/2}(p_{1/2})^{-2}$ at $E_x=12.86$ and 12.66 MeV, respectively. These states will be excited selectively by one-nucleon stripping reactions such as the $^{14}\text{N}(d,p)^{15}\text{N}$ reaction. However, no experimental data for one-nucleon stripping reactions have been reported yet in the region of such high excitation energy in ^{15}N . As seen in Table II, states with similar two-nucleon configurations have a fairly good correspondence between ^{14}N and ^{15}N in terms of their spectroscopic strengths and their locations in excitation energy, where the 1^- , 5.69 MeV and the 3^- , 5.83 MeV states in ^{14}N have their corresponding two $\frac{1}{2}^+$ states and two $\frac{5}{2}^+$ states in ^{15}N , respectively, reflecting the degree of freedom of $T=0$ and 1 components in $(p)^{-2}$ coupling. Our proposal is that the $\frac{5}{2}^+$, 12.33 MeV and the $\frac{3}{2}^+$, 13.83 MeV states in ^{15}N may have the $d_{3/2}(p_{1/2})^{-2}$ configuration owing to the next two points: (1) The cross sections for these states should be larger than those for the adjacent states, due to their simple structure of $d_{3/2}(p_{1/2})^{-2}$. (2) They should be located around $E_x=12$ MeV corresponding to the excitation energy of 9.39 MeV for the 2^- state in ^{14}N , as expected from the energy spacing between the 2^- , 9.13 MeV state in ^{14}N and the $\frac{5}{2}^+$, 12.10 MeV state in ^{15}N . The recent compilation¹ lists the spin for the 12.33 MeV state as $J=\frac{5}{2}$, but the parity is not established. If the parity for the 12.33 MeV state were negative, the transferred angular momentum for the state should be $L=2$. The experimental shape for an $L=2$ transfer exhibits a rather flat shape at forward angles, as seen from the cross sections for the 12.56 MeV state in Fig. 3. The rise in the shape at forward angles seen in Fig. 4 for the 12.33 MeV state is a characteristic of $L=1$ transfer, which is consistent with the shape for the corresponding 2^- state in ^{14}N . Thus, the assignment of $J^\pi=\frac{5}{2}^+$ to the 12.33 MeV state is preferred.

The lowest $\frac{7}{2}^+$ state at $E_x=7.56$ MeV is described as having the simple configuration $(d_{5/2})[(p_{1/2})_{1+;T=0}^{-2}]$ in

the weak coupling model.³ Previously the configuration was confirmed by several authors^{7,8} via the $^{12}\text{C}(\alpha, p)^{15}\text{N}$ reaction. Our result also supports the configuration; a reasonable fit of the calculated curve to the cross section as well as the enhancement factor consistent with that for the corresponding 3^- , 5.83 MeV state in ^{14}N are seen in Fig. 4 and in Table II.

According to the weak coupling model,³ the $\frac{9}{2}^+$, 10.69 MeV state has a structure of 3p-4h. The structure was confirmed via the $^{12}\text{C}(\alpha, p)^{15}\text{N}$ reaction.^{7,8} The reaction $^{13}\text{C}(\alpha, d)^{15}\text{N}$ cannot excite a state with such a configuration. As seen in Fig. 3, the present cross section for the doublet¹ of the $\frac{9}{2}^+$, 10.69 MeV and the $\frac{3}{2}^-$, 10.70 MeV states in ^{15}N is well reproduced with an $L=0$ curve. Namely, the cross section is due only to the transition to the $\frac{3}{2}^-$, 10.70 MeV state.

B. High-spin states with a $(d_{5/2})^2$ configuration in ^{14}N and ^{15}N

The 5^+ 8.96 and 10.81 MeV states in ^{14}N have a stretched configuration of $(d_{5/2})^2_{5^+}$.¹⁴ The satisfactory fit of the calculated curve to the data for these 5^+ states also supports their simple two-nucleon configuration. Previously, Lie¹⁴ pointed out that most of the strength for the $(d_{5/2})^2_{5^+}$ configuration is concentrated in the lowest 5^+ state for an interaction of a Gillet type without a tensor force, and that the distribution of the strength between these 5^+ states depends sensitively on the effective two-nucleon interaction of the tensor type. Thus the comparison of the strengths for these 5^+ states would provide some information on the tensor interaction between two nucleons in the $0d_{5/2}$ shell. As listed in Table III, the enhancement factors for these 5^+ states are nearly the same, contradicting the prediction. Thus our data may support the introduction of a tensor interaction for the 5^+ stretched two-particle states. At the present incident energy, an estimation on a contribution from complicated reaction processes other than a direct deuteron transfer may be needed in order to get reliable spectroscopic information on the transition to these 5^+ states. Such an effect of the reaction processes is seen in the cross section for the $\frac{11}{2}^-$ state in ^{15}N .

Contrary to these high spin states in ^{14}N , cross sections for the known $\frac{11}{2}^-$, 13.00 MeV and the $\frac{9}{2}^-$, 11.94 MeV states in ^{15}N show sharp rises at forward angles as seen in Fig. 3. At the higher incident energy of 40 MeV, the cross sections for the (α, d) transition to the 13.00 and the 11.94 MeV states are reported to have shapes similar to those for the 5^+ , 8.96 MeV state in ^{14}N .⁴ Thus the (α, d) transition to these states seems to have an energy dependence around $E_{\text{lab}}=35$ MeV. In spite of such ambiguity, the enhancement factor for the $\frac{11}{2}^-$, 13.00 MeV state has a reasonable value in comparison with that for the 8.96 MeV state in ^{14}N .

On the other hand, the strength for the $\frac{9}{2}^-$, 11.94 MeV state is smaller than that for the $\frac{11}{2}^-$ state, indicating the escape of the strengths for the $[(d_{5/2})^2_{5^+}p_{1/2}]_{9/2^-}$ configuration to the other $\frac{9}{2}^-$ state as predicted by Lie *et al.*³

The recent compilation¹ mentions the possibility of $J=\frac{9}{2}$ for the 12.56 and 13.17 MeV states in ^{15}N . As seen in Fig. 3(b), the shape of the cross section for the 12.56 MeV state is different from that for the 11.94 MeV $\frac{9}{2}^-$ state and also from the calculated curve with $L=4$ transfer. In the figure, it is reproduced with an $L=2$ curve. The cross section is about $\frac{1}{3}$ of that for the 11.94 MeV state. Recently Hamill *et al.*⁷ studied the $^{12}\text{C}(\alpha, p)^{15}\text{N}$ reaction and found that the (α, p) transition to the $\frac{11}{2}^-$, 13.00 MeV and the $\frac{9}{2}^-$, 11.94 MeV states shows shapes of angular distributions as predicted by a simple DWBA calculation, suggesting the suitability of the (α, p) reaction for studying high spin states in ^{15}N . Another of their findings suggests that the 12.56 MeV state is similar to the $\frac{9}{2}^-$, 11.94 MeV state both in shapes of the cross sections and in their strengths. On the other hand, the cross section for the 13.17 MeV state is much flatter in shape and smaller by a factor of 2 than those for the 11.94 and 12.56 MeV states. Thus, they proposed an assignment of $J^\pi=\frac{9}{2}^-$ to the 12.56 MeV state. The (α, p) transition is allowed access to a state of $(d_{5/2})^2_{4^+;1}$ as well as to that of $(d_{5/2})^2_{5^+;0}$. Hence, combining the results for the $^{12}\text{C}(\alpha, p)^{15}\text{N}$ reaction and the $^{13}\text{C}(\alpha, d)^{15}\text{N}$ reaction, one can propose that the main configurations of the 11.94 and 12.56 MeV states are $(d_{5/2})^2_{5^+;0}$ and $(d_{5/2})^2_{4^+;1}$, respectively, and that the mixing between these configurations is small, contrary to Lie's calculation. The small mixing seems to indicate the necessity of the introduction of a more realistic two-nucleon interaction in order to understand these high spin states with a $(d_{5/2})^2$ configuration. The seeming $L=2$ shape for the (α, d) transition to the 12.56 MeV state may come from the higher order components of the complex configurations in the state.

C. Effects of a multistep process via $^{12}\text{C}(2^+)$

The 1^- , 5.69 MeV state in ^{14}N is described to be of $s_{1/2}(p_{1/2})^{-3}$ configuration in the weak coupling shell model.¹⁴ The shape of the angular distribution for the 1^- state is much different at forward angles from the DWBA calculation. In order to explain the abnormal shape, contributions of the two-step process via the 2^+ state of ^{12}C have been estimated by using the program CHUCK.²⁹ Figure 5 is the result where a deformation parameter $\beta_2=-0.40$ (Ref. 30) is used for a real coupling between the ground and the 2^+ state in ^{12}C . One-way couplings are assumed in the calculation in order to eliminate effects of nonorthogonal terms³¹ in the zero-range DWBA calculation for the (α, d) transition. Macroscopic form factors are used by assuming the leading configuration for the transfer from the 2^+ state in ^{12}C to the 1^- state in ^{14}N to be $s_{1/2}p_{3/2}$. The (NLJ) values used are $(NLJ)=(111)$ for $^{12}\text{C}(\alpha, d)^{14}\text{N}(1^-)$ and $(NLJ)=(112)$ for the (α, d) transition from $^{12}\text{C}(2^+)$ to $^{14}\text{N}(1^-)$. In the figure, a broken curve and a dotted curve represent the one-step and the two-step contributions, respectively. The solid curve is the coherent sum of these two terms. In spite of the simplified treatment, the general behavior of the angular distribution is well reproduced by the calculation. Thus one

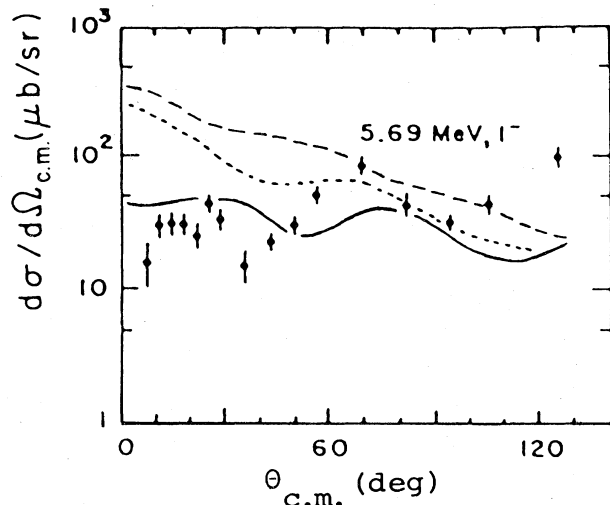


FIG. 5. Angular distributions for the $^{12}\text{C}(\alpha,d)^{14}\text{N}$ reaction leading to the 5.69 MeV states. Broken curves; one-step process for the (α,d) reaction. Dotted curves; two-step process preceded by inelastic scattering to the 2^+ , 4.44 MeV state in ^{12}C , where one-way coupling and $\beta_2 = -0.4$ are assumed. Solid curves; coherent sum of the above two processes. See also the explanation in the text.

can point out that the two-step process via the 2^+ state in ^{12}C plays an important role for the (α,d) transitions to the 1^- state.

V. SUMMARY

In the present work on the (α,d) reaction on ^{12}C and ^{13}C , several new facts are found.

(i) At the incident energy of 35 MeV, nondirect processes have been observed in some of the angular momentum mismatched transfer of $L=0, 1,$ and 2 . The states in ^{14}N for which cross sections show shapes different from DWBA predictions are considered in the shell model calculations^{14,32} to have amplitudes based on the 2^+ , 4.44 MeV state in ^{12}C . Besides, at this incident energy, the $^{12}\text{C}(\alpha,\alpha)^{12}\text{C}$ scattering is matched for the $L=2$ transfer to the 2^+ state in ^{12}C . These two factors provide reasons why some of the angular distributions for the (α,d) reaction demonstrate abnormal shapes compared to those for the corresponding $(^3\text{He},p)$ reaction.^{11,26} As an example of the effect of the two-step process, the cross section for the 1^- , 5.69 MeV state in ^{14}N is analyzed in the framework of the second order DWBA. On the other hand, for the momentum matched transfers of $L=3$ and 4 , reasonable fits of DWBA calculations alone to the data are found by using a deuteron-cluster form factor, except for the transition to the $\frac{11}{2}^-$, 13.00 MeV and the $\frac{9}{2}^-$, 11.94 MeV states in ^{15}N . In order to understand the problem evident in the transition to the $\frac{11}{2}^-$ and $\frac{9}{2}^-$ states, excitation functions for the $^{13}\text{C}(\alpha,d)^{15}\text{N}$ reaction should be measured around $E_\alpha = 35$ MeV. In spite of several ambiguities in the DWBA analyses of the present data, the (α,d) reaction has been found to be suited for observing the component of

the two-particle configurations from states with a mixture of $1p$ - $2h$ and $3p$ - $4h$ structure in ^{15}N .

(ii) By comparing the available spectroscopic data with the weak coupling shell model calculation,^{3,14} effects of the $0d_{3/2}$ shell are found in the 2^- , 9.39 MeV state in ^{14}N and in the $\frac{5}{2}^+$, 12.33 MeV and $\frac{3}{2}^+$, 13.83 MeV states in ^{15}N . Their possible configurations are proposed to be $[d_{3/2}(p_{1/2})^{-3}]_{2-}$ and $[d_{3/2}(p_{1/2})^{-2}]_{5/2+3/2+}$, respectively. The obtained enhancement factor for the $d_{3/2}p_{1/2}$ configuration is smaller than that for the $d_{5/2}p_{1/2}$ configuration. Hence, the other states with a $0d_{3/2}$ component seem to be distributed in the region of higher excitation energy.

(iii) Around $E_x = 10$ MeV in ^{14}N and ^{15}N , $0p_{1/2}$, $0p_{3/2}$, $0d_{5/2}$, $0d_{3/2}$, and $1s_{1/2}$ shells are all active. This leads to a speculation that the two-nucleon configurations for the highly excited states may be sensitive to the effective interactions used in the shell model calculation. The present work shows the following characteristics of the states with a stretched $(d_{5/2})^2$ configuration: The enhancement factor for the second 5^+ state in ^{14}N is about 80% of that for the first 5^+ state, much different from Lie's prediction.¹⁴ Besides, the cross section for the second $\frac{9}{2}^-$, 12.56 MeV state in ^{15}N is only $\frac{1}{3}$ of that for the first $\frac{9}{2}^-$, 11.94 MeV state, and different in shape from the latter. From the comparative study of the (α,d) and (α,p) transitions to these $\frac{9}{2}^-$ states, the leading configurations seem to be $(d_{5/2})^2_{5+;0}$ and $(d_{5/2})^2_{4+;1}$, respectively, and the mixing between the configurations seems to be small, contrary to the prediction in the weak coupling shell model calculation.³ Previously, Lie¹⁴ suggested the importance of the tensor force for the stretched 5^+ states in ^{14}N , but took no account of the force in his actual calculation. These discrepancies for the stretched configurations between the obtained results and the prediction may indicate the necessity for the introduction of the tensor force to the effective two-nucleon interaction in these nuclei.

(iv) For the $\frac{1}{2}^+$ states in ^{15}N , the enhancement factor for the $\frac{1}{2}^+$, 5.30 MeV state demonstrates a considerable discrepancy from the prediction in the weak coupling shell model calculation.³ Harwood and Kemper²⁷ also pointed out the insufficiency of the model to describe the electromagnetic properties of the $\frac{1}{2}^+$ states in ^{15}N .

This comparative study of the (α,d) reaction on ^{12}C and ^{13}C has revealed much of the shell structure of the states in ^{14}N and ^{15}N , and demonstrated some deviations from the weak coupling shell model calculations.^{3,14} In the shell model calculation of these nuclei, it seems that a more realistic effective interaction such as investigated by Millener and Kurath²⁸ is needed.

ACKNOWLEDGMENTS

The authors are grateful to Prof. D. A. Lind and Prof. C. D. Zafiratos for their encouragement throughout the work. Some of the numerical calculations were carried out with the central computer at the Institute for Nuclear Study (INS).

- *Present address: Institute for Nuclear Study, University of Tokyo, Tokyo 188, Japan.
- † Present address: Kernfysich Versneller Instituut, 9747 AA Groningen, The Netherlands.
- ‡ Present address: Department of Physics, Seoul National University, Seoul, Republic of Korea.
- ¹F. Ajzenberg-Selove, Nucl. Phys. **A360**, 1 (1981).
- ²W. Kretschmer, G. Probstle, and W. Stach, Nucl. Phys. **A333**, 13 (1980).
- ³S. Lie, T. Engeland, and G. Dahll, Nucl. Phys. **A156**, 449 (1970); S. Lie and T. Engeland, *ibid.* **A169**, 617 (1971); **A267**, 123 (1976).
- ⁴C. C. Lu, M. S. Zisman, and B. G. Harvey, Phys. Rev. **186**, 1086 (1969).
- ⁵L. H. Harwood and K. W. Kemper, Phys. Rev. C **16**, 1040 (1977).
- ⁶S. Cohen and D. Kurath, Nucl. Phys. **A101**, 1 (1967).
- ⁷J. J. Hamill, Ph.D. thesis, University of Colorado, 1982 (unpublished); J. J. Hamill, R. J. Peterson, and M. Yasue, Nucl. Phys. **A408**, 21 (1983).
- ⁸W. R. Falk, A. Djaloeis, and D. Ingham, Nucl. Phys. **A252**, 452 (1975).
- ⁹A. F. Zeller, K. W. Kemper, T. R. Ophel, and A. Johnston, Nucl. Phys. **A344**, 307 (1980).
- ¹⁰R. H. Pehl, E. Rivet, J. Cerny, and B. G. Harvey, Phys. Rev. **137**, B114 (1965); E. Rivet, R. H. Pehl, J. Cerny, and B. G. Harvey, *ibid.* **141**, 1021 (1966).
- ¹¹N. F. Mangelson, B. G. Harvey, and N. K. Glendenning, Nucl. Phys. **A117**, 161 (1968).
- ¹²A. van der Woude and R. J. de Meijer, Nucl. Phys. **A258**, 199 (1976).
- ¹³R. L. White, L. A. Charlton, and K. W. Kemper, Phys. Rev. C **12**, 1918 (1975).
- ¹⁴S. Lie, Nucl. Phys. **A181**, 517 (1972).
- ¹⁵B. W. Ridley, D. E. Prull, R. J. Peterson, E. W. Stoub, and R. A. Emigh, Nucl. Instrum. Methods **130**, 79 (1975).
- ¹⁶D. E. Prull, computer code SPECTR, University of Colorado (unpublished).
- ¹⁷M. Yasue, J. J. Hamill, H. C. Bhang, M. A. Rumore, and R. J. Peterson, Institute of Nuclear Study Report 488, 1984.
- ¹⁸R. J. de Meijer, L. W. Put, and J. C. Vermeulen, Phys. Lett. **107B**, 14 (1981); R. J. de Meijer, L. W. Put, J. J. Akkerman, J. C. Vermeulen, and C. R. Bingham, Nucl. Phys. **A386**, 200 (1982).
- ¹⁹Y. Kadota, K. Ogino, Y. Nishibori, K. Obori, Y. Taniguchi, M. Yasue, and J. Schimizu, Institute for Nuclear Study (Tokyo) Annual Report, 1978, p. 37.
- ²⁰P. D. Kunz (unpublished).
- ²¹R. R. Sercely, R. J. Peterson, P. A. Smith, and E. R. Flynn, Nucl. Phys. **A324**, 53 (1979).
- ²²R. M. Del Vecchio, R. T. Kouzes, and R. Sherr, Nucl. Phys. **A265**, 220 (1976).
- ²³R. M. Del Vecchio and W. W. Daehnick, Phys. Rev. C **6**, 2095 (1972).
- ²⁴J. D. Cossair, W. S. Burns, and R. A. Kenefick, Nucl. Phys. **A287**, 13 (1977).
- ²⁵R. J. Peterson and J. J. Hamill, Nucl. Phys. **A362**, 163 (1981).
- ²⁶T. Pederson, T. Engeland, I. Espe, J. Rekstad, C. Ellegaard, and S. Backe, Nucl. Phys. **A293**, 10 (1977).
- ²⁷L. H. Harwood and K. W. Kemper, Phys. Rev. C **20**, 1383 (1979).
- ²⁸D. J. Millener and D. Kurath, Nucl. Phys. **A255**, 315 (1975).
- ²⁹P. D. Kunz (unpublished).
- ³⁰M. Yasue, T. Tanabe, F. Soga, J. Kokame, F. Shimokoshi, J. Kasagi, Y. Toba, Y. Kadota, T. Ohsawa, and K. Furuno, Nucl. Phys. **A394**, 29 (1983).
- ³¹M. Igarashi, Phys. Lett. **78B**, 379 (1978).
- ³²S. Cohen and D. Kurath, Nucl. Phys. **A141**, 145 (1970).